

Article

A Comparative Study of Malonic and L-Glutamic Acids for Metal Leaching from Spent Lithium-Ion Batteries: Kinetic and Optimization Analysis

Laleh Sohbatzadeh ¹, Sied Ziaedin Shafaei Tonkaboni ^{1,*}, Mohammad Noaparast ¹ and Ali Entezari-Zarandi ² 

¹ School of Mining Engineering, Faculty of Engineering, University of Tehran, Tehran 1439957131, Iran; sohbatzadeh.l@ut.ac.ir (L.S.)

² Hecla Québec, Rouyn-Noranda, QC J9Z 2Y9, Canada; aezarandi@hecla.com

* Correspondence: zshafaie@ut.ac.ir

Abstract: In this research, two different hydrometallurgical processes were introduced for recycling the cathodes of lithium-ion batteries (LIBs) from spent LIBs. The cathode materials were leached by malonic acid (MOA), as a leaching agent, and ascorbic acid (AA), as a reducing agent, in the first process, and by L-Glutamic acid (L-Glu), as a leaching agent, and AA, as a reducing agent, in the second process. The results of the tests showed that, with a similar solid-to-liquid (S/L) ratio of 10 g/L and a recovery time of 2 h for both processes, when using MOA of 0.25 M and AA of 0.03 M at 88 °C, 100% lithium (Li), 80% cobalt (Co), 99% nickel (Ni), and 98% manganese (Mn) were extracted, and when using L-Glu of 0.39 M and AA of 0.04 M at 90 °C, 100% Li, 79% Co, 91% Ni, and 92% Mn were extracted. The kinetics of the leaching process for the two systems were well justified by the Avrami equation, which was diffusion-controlled in the MOA + AA system, with the apparent activation energy of 3.23, 14.72, 7.77, and 7.36 kJ/mol for Mn, Ni, Co, and Li, respectively. The L-Glu + AA involved chemical-diffusion kinetic control, with the apparent activation energy for Mn, Ni, Co, and Li of 9.95, 29.42, 20.15, and 16.08 kJ/mol, respectively. Various characterization techniques were used to explain the observed synergistic effect in the L-Glu + AA system, which resulted in reduced acid consumption and enhanced recovery compared to the case of MOA + AA. This occurred because L-Glu is not able to reduce and recover metals without a reductant, while MOA has reductant properties.

Keywords: lithium-ion battery recovery; leaching kinetics; malonic acid; L-Glutamic acid; leaching optimization



Citation: Sohbatzadeh, L.; Shafaei Tonkaboni, S.Z.; Noaparast, M.; Entezari-Zarandi, A. A Comparative Study of Malonic and L-Glutamic Acids for Metal Leaching from Spent Lithium-Ion Batteries: Kinetic and Optimization Analysis. *Minerals* **2023**, *13*, 1104. <https://doi.org/10.3390/min13081104>

Academic Editor: Jean-François Blais

Received: 20 June 2023

Revised: 7 August 2023

Accepted: 17 August 2023

Published: 19 August 2023



Copyright: © 2023 by the authors. Licensee MDPI, Basel, Switzerland. This article is an open access article distributed under the terms and conditions of the Creative Commons Attribution (CC BY) license (<https://creativecommons.org/licenses/by/4.0/>).

1. Introduction

LIBs are extensively applied in devices such as portable electronic equipment as well as hybrid/electric vehicles worldwide due to their excellent electrochemical performance at high voltage, high energy density, low discharge, low memory effect, good stability cycle and long life [1–3].

Electric vehicles may play an important role in sustainable environmental development goals to reduce air pollution and climate change [4–6]. In the future, sales of electric vehicles are expected to significantly grow to 18 million in 2025 and 21 million in 2030 [3,7]. According to a report by the International Energy Agency (IEA), the global electric car stock will rise to 50 million by 2025 and 140 million by 2030 [2]. Electric cars are powered by one or more electric motors connected to a grid and store the electricity in batteries [4]. The inevitable use of LIBs leads to the mass production of spent LIBs and demand for various cathodic materials in them [8]. The market for LIBs is growing rapidly, providing an efficient way to store renewable energy and reduce dependence on fossil fuels [9,10].

Spent LIBs consist of a positive electrode (cathode during discharge), organic solvent, diaphragm, negative electrode (anode during discharge), shell and electrolyte that contain

Co, Mn, Li, Ni, copper (Cu), aluminum (Al) and other heavy metals [11]. Due to such toxic heavy metals, the unsuitable disposal of spent LIBs in nature may harm the environment, pollute soil and groundwater, and ultimately threaten human health [12,13], while recycling spent LIBs causes the reuse of valuable metals, including Co, Mn, Li and Ni, etc. [13]. Depending on the type of battery, the average LIB contains 5–20 wt% of Co and Ni, 5–15 wt% of Mn, 5–10 wt% of Cu and 5–7 wt% of Li [14]. The grade of these metals is much higher in comparison with the natural raw ore; therefore, proper operation and recycling of valuable metals from LIBs are useful for environmental protection and the recycling of resources [15].

Hydro- and pyrometallurgical processes are the two main methods for recycling spent LIBs. Pyrometallurgy is often faster while having disadvantages such as high energy consumption, low purity of recycled materials and large investment [16]. Pyrometallurgical processes involve high temperatures (i.e., often >1000 °C) [9]. Although the pyrometallurgical process is simple, it requires large investments in equipment [11]. The products usually consist of Ni, Co, Cu, iron (Fe) alloys and Mn, Al and Li slags [17]. Li remains in the slag and is difficult to recycle due to its high reactivity [18]. Compared with the pyrometallurgy process, the hydrometallurgical process has higher recovery efficiency and product purity, as well as lower cost and energy consumption. The main steps in the hydrometallurgical processes for recycling spent LIBs include size reduction, dismantling, leaching and physical separation [19,20]. Leaching is an essential step in which leaching agents, pH and oxidation/reduction potential modifiers play important roles in the efficiency, selectivity and energy consumption [21,22].

Compared with mineral acids (e.g., HCl [23], H₂SO₄ [24] and H₃PO₄ [25]), leaching with organic acids (such as ascorbic acid [26], acetic acid [27], citric acid [8] and oxalic acid [28]) is widely conducted in the recovery of valuable metals because it does not produce too much acidic wastewater and does not cause the corrosion of equipment [29]. Mineral acid leaching leads to toxic emissions such as SO₃, Cl₂ and NO_x, resulting in significant secondary contamination [30]. Although a similar leaching efficiency is obtained for both organic and mineral acids, organic acids are preferred due to less environmental pollution during leaching. However, a high concentration of organic acids is often required for the complete dissolution of the LIB cathode when only one organic acid is the leaching agent [31]. In several studies, it was confirmed that when different organic acids are used simultaneously in the leaching process, the acid consumption can be considerably reduced [32]. Table 1 shows a set of mixed acid leaching systems.

Table 1. Summary of some mild organic acids mixed in leaching for the recycling of spent LIBs [32].

Leaching Reagents	Conditions	Sample	Leaching Efficiency (%)
0.4 M tartaric acid + 0.02 M ascorbic acid	5 h; 80 °C	LiCoO ₂	Li: 99.5%; Co: 95%
0.5 M glycine + 0.02 M ascorbic acid	6 h; 80 °C	LiCoO ₂	Co: 95%
0.1 M nitrilotriacetic acid + 0.02 M ascorbic acid	6 h; 80 °C	LiCoO ₂	Li: 96%; Co: 75%
0.1 M adipic acid + 0.02 M ascorbic acid	6 h; 80 °C	LiCoO ₂	Li: 92%; Co: 85%
0.2 M phosphate acid + 0.4 M citric acid	0.5 h; 90 °C	LiNi _{0.5} Co _{0.2} Mn _{0.3} O ₂	Li: 100%; Ni: 93.4%; Co: 91.6%; Mn: 92%

In the leaching process, reducing agents such as hydrogen peroxide (H₂O₂) [9,11,13], sodium bisulfite (NaHSO₃) [33], sodium sulfite (Na₂SO₃) [5], glucose [34] and AA [12,24] are added to increase the leaching recovery. All of these chemicals increase the Co dissolution by reducing Co⁺³ to Co⁺². However, the production of some chemical reductants

causes certain pollution to the environment [35]. Therefore, finding a leaching system with mild operating conditions, low impact on the environment, and low acid consumption, as well as ensuring high leaching efficiency, is essential.

Determination of the leaching kinetics in hydrometallurgical studies is required to determine the regulatory steps in the process [36]. Thus far, different models have been proposed to describe the solubility–extraction reactions through the S/L ratio interactions. Two of the most widely used are the shrinking particle model (SPM) and the shrinking core model (SCM) [37,38]. The Avrami equation is another combined kinetic equation that includes the diffusion control and chemical reaction used in heterogeneous solid–liquid systems [36,39,40].

The present research focuses on the leaching process and the recovery of valuable metals from spent LIBs, so that the aim of this study is to investigate the leaching kinetics for the recovery of Mn, Co, Ni and Li from the cathodes of spent LIBs. In this study, for the first time, the combination of an organic acid (MOA or L-Glu) as a leaching agent and AA as a reducing agent are used for leaching. The advantages of this study include the use of MOA and L-Glu, which are biodegradable, water-soluble and environmentally friendly acids [41,42]. Moreover, these two dicarboxylic acids have high acidic strength compared to other organic acids due to their two functional carboxyl groups (-COOH). The synergistic effect of acids mixed in the leaching process may have affected the acid consumption, causing less acid to be used, resulting in a lower cost of leaching. Additionally, AA was used as an effective reducing agent due to its efficient Ni and Co reduction into their highest state, which resulted in enhancing the leaching process in an acidic solution.

2. Materials and Experiments

2.1. Materials

Approximately, 77 spent LIBs from laptops were collected from different local electronics stores. After undergoing a 2 h calcination, approximately 0.1 g of the spent battery's cathode powder was completely dissolved in 20 mL of aqua regia (HNO₃: HCl = 1:3, *v/v*) and the content of various metals in the solution was determined via atomic absorption spectroscopy. The battery's cathode active materials contained 5.86% Li, 32.21% Co, 12.73% Ni and 10.57% Mn. Elemental analysis of the spent LIB cathode via XRF for pre- and post-200 mesh sieving and after 2 h of calcination is provided in Table 2. Due to the existence of L.O.I. in the XRF analysis, the values obtained are slightly different from the results from AAS. The purpose of the XRF analysis is to offer readers a general overview of the elements in the cathode sample.

Table 2. Elemental analysis of an LIB cathode (before and after 200 mesh sieving and after 2 h of calcination).

The Chemical Elements in Cathode Material of the LIB	Retained Particles	Passed Particles	2 h Furnace
Al (wt%)	23.73	0.59	0.58
K (wt%)	0.07	-	0.07
Ni (wt%)	8.35	14.30	15.01
Si (wt%)	0.14	0.09	0.11
Ca (wt%)	0.09	-	-
P (wt%)	0.10	0.20	0.19
Mn (wt%)	5.97	8.10	10.51
S (wt%)	0.02	0.07	0.06
Co (wt%)	15.80	34.66	36.27
Mg (wt%)	-	-	0.11
L.O.I.	8.18	9.35	1.90

The leaching agents included MOA ($C_3H_4O_4$) and L-Glu ($C_5H_9NO_4$), and AA ($C_6H_8O_6$) was used as the reducing agent. All the reagents were of analytical grade and were obtained from Merck, except for nitric acid (HNO_3 , 65%) and hydrochloric acid (HCl , 37%), which were purchased from Mogilalia Company (Iran). All the solutions were prepared using distilled water.

2.2. Analytical Methods

2.2.1. Instrumental Methods

The cathode material was dissolved in aqua regia for 24 h prior to the metal concentration analysis via atomic absorption spectrometry (ASS, Varian AA220FS, Australia). The crystalline structure of the cathode powder, the residue after leaching, and the carbon existence after calcination were investigated using an X-ray diffractometer (XRD, Philips-3040/60 PW) with Cu-K α radiation operated at 40 kV, and 40 mA and the data ranged from $5^\circ \leq 2\theta \leq 100^\circ$. A sequential X-ray fluorescence spectrometer (XRF, ARL PERFORM'X) was used for the chemical composition analysis of the cathode powder before and after sieving and after calcination. However, XRF is limited to the atomic numbers of elements, and low atomic numbers and energies such as Li, carbon, and oxygen are not detected via XRF. Scanning electron microscopy (SEM, HITACHI S-4160) and energy dispersive X-ray spectroscopy (SAMx, DXP-XIOP, France) were used to analyze the surface morphology and determine the elemental distribution map on the surface of the active materials before and after leaching. The FT-IR spectrum was recorded by the spectrometer (Thermo Nicolet Nexus 870 ESP FT-IR, USA) using a KBr pellet. The UV-Vis spectrum from the leaching was recorded using a UV-Visible spectrophotometer (Thermo Biomate 5 UV-Visible Spectrophotometer, Florida, USA) to investigate the synergistic effect of the acids.

2.2.2. Chemical Methods

The leaching efficiency of the metal contents of the cathode materials was calculated using the following equation:

$$R(\%) = \left(1 - \frac{G_w \times W_w}{G_f \times W_f}\right) \times 100 \quad (1)$$

where R is the leaching efficiency (%), G_w is the element grade of the residual leached powder (%), W_w is the weight (g) of the residual leached powder, G_f is the element grade in the cathode (%) and W_f is the cathode weight (g).

2.3. Leaching Methods

Prior to leaching, it is necessary to remove any carbon and organic compounds to reduce the acid consumption. First, the spent LIBs were dipped in a saturated NaCl solution (5 wt%) for 24 h to discharge them and prevent any potential spontaneous combustion or short circuit explosion [21,43]. After drying, the metal shell of the battery was removed and the anode and cathode were manually separated [44]. Each LIB cell, the cathode material, the anode material, the separator and the metal shell weighed 43 g, 19 g, 11 g, 2 g and 7 g, respectively. The cathode material was cut into small parts (about 1 cm \times 1 cm) and dried at 60 $^\circ C$ for 24 h in the oven. The cathode shredding was further processed through 2 h of ball milling. To avoid impurities in the cathode materials, a ceramic-walled ball mill was used. The resulting powder was subsequently sieved (both dry and wet) to obtain a product of 100% below 75 μm , which was divided into 2 parts using a riffle splitter. Finally, the black cathode powder was heated at 700 $^\circ C$ for 2 h in the furnace to remove any carbon and polyvinylidene fluoride (PVDF).

All the experiments were conducted using a PYREX Flask Erlenmeyer 500 mL (ISO Lab, Eschau, Germany) containing 100 mL of experiment solution. To avoid any change in the temperature of the experiment environment, the Erlenmeyer was placed inside a water bath and the temperature was controlled by a glass thermometer in the error

variation of ± 5 °C. In order to reduce the evaporation, a glass condenser was placed on the Erlenmeyer. A magnetic stirrer was used to mix and stir the solution. All the experiments were conducted in 2 h, and the S/L ratio of all the tests was 10 g/L. As the final step in each experiment, the solution was filtered using filter paper (150 mm, Whatman International Ltd. Maidstone, Hangzhou, China) and washed with distilled water.

2.4. Process Optimization

For an optimized leaching process, the 2-level fractional factorial design method was used to remove the statistically insignificant parameters. Then, using Central Composite Design, the experiments were optimized using the Demo version of Design Expert 12 (State-Ease Inc., Minneapolis, MN, USA). The parameters and their levels that were identified as potentially influential in terms of the leaching efficiency, such as the reaction time (2–8 h), temperature (30–90 °C), S/L ratio (1–10 g/L), acid type (MOA, L-Glu), acid concentration (0.1–0.5 M) and reducing agent concentration (0.01–0.05 M), were determined based on a literature review [45–47].

Following the completion of the test works, half-normal plot and Pareto charts were used to identify the effective parameters, where the leaching time and S/L ratio were found to be insignificant parameters. Therefore, during the optimization experiments, an S/L ratio of 10 g/L and a leaching time of 2 h were considered.

In the following step, due to its high accuracy, the response surface methodology (RSM) was applied to optimize the effective parameters (acid type and concentration, reducing agent concentration and temperature) in the recovery of Co, Mn, Li and Ni. While the applied software is known for its high accuracy, it is important to acknowledge that certain errors, such as those associated with metal quantification with AAS, undesired evaporation during the leaching process, volumetric measurements, and dilution coefficients, would have affected the test results in practice and should not be disregarded. To avoid additional explanations, the results of the variance analysis are mentioned in [48].

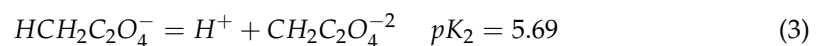
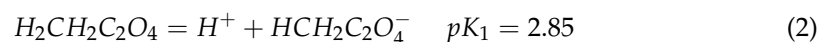
3. Results and Discussion

3.1. Leaching Conditions

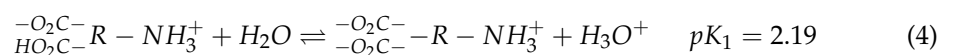
3.1.1. Effect of Organic Acid on the Leaching Process

Figure 1a shows the effect of the acid type (L-Glu and MOA) on the recovery of Ni, Co, Li and Mn via leaching with an acid concentration of 0.39 M, an AA concentration of 0.04 M and at the temperature of 90 °C. By changing the organic acid from L-Glu to MOA, the recovery increased from 89.51% to 100% for Li, from 77.91% to 92.28% for Co, from 85.71% to 100% for Ni and 92.30% to 99.91% for Mn. MOA was more effective than L-Glu and found to be a better leaching agent because of its higher water solubility.

The reaction of MOA dissociation is as follows: [42]



Moreover, the reaction of L-Glu dissociation, which is an amino acid, is as follows: [49]



These equations show that L-Glu and MOA have a two-step dissociation reaction, from which two H^+ moles are produced. According to studies, MOA is more likely to be efficient than L-Glu. Considering the molecular structure of both acids (MOA ($CH_2(COOH)_2$) and L-Glu ($HOOC-CH(NH_2)-(CH_2)_2-COOH$)), both are composed of two carboxylic groups [48]. However, the acidic strength of L-Glu decreases with the existence of an

amine group as well as an increased length of the carbon chain in the structure of L-Glu. Furthermore, the intramolecular hydrogen bonds between the acid group and the amine contribute to the reduction in the acidic properties [42,49,50].

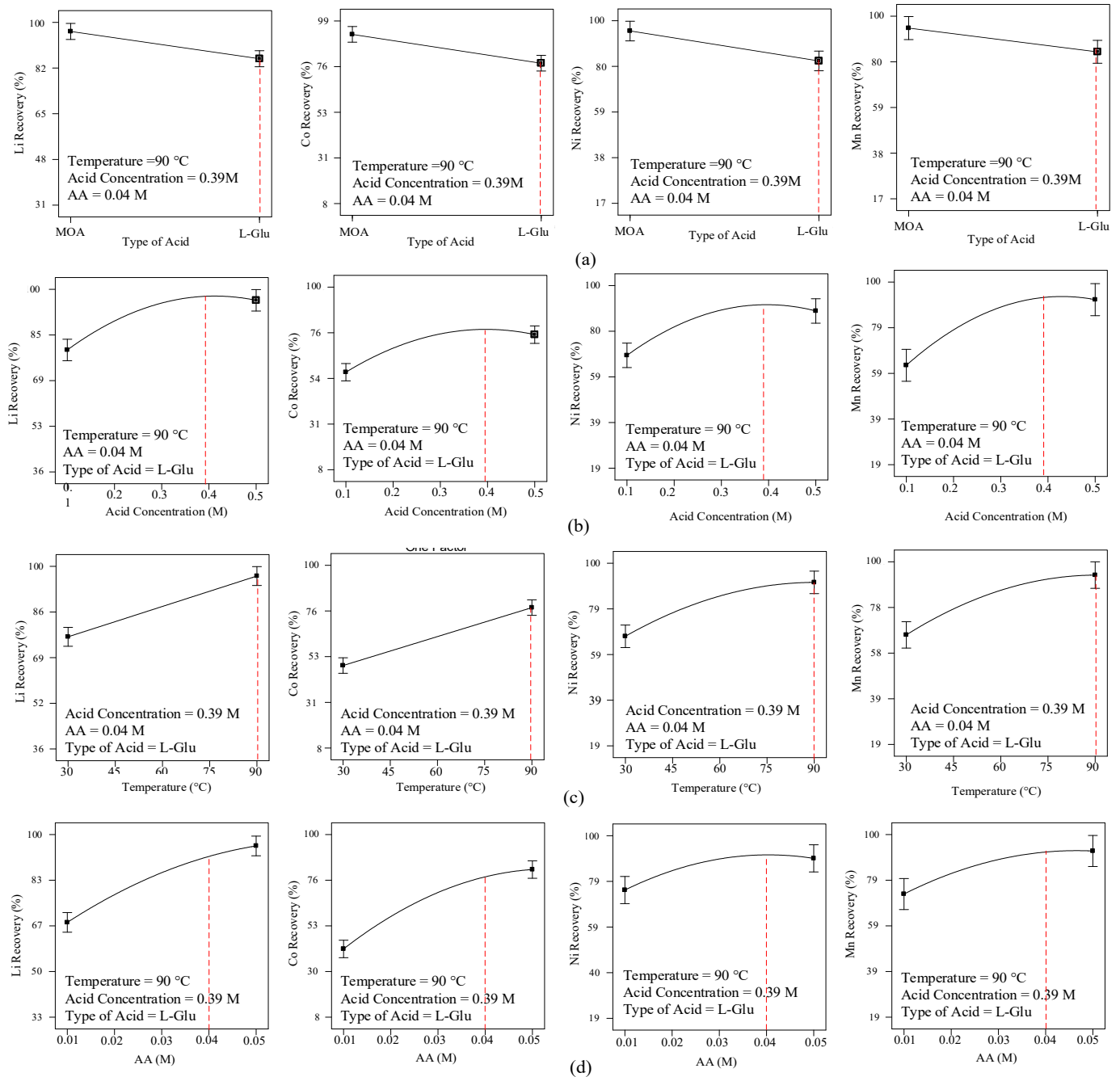


Figure 1. Effect of the leaching parameters on Li, Co, Ni and Mn: (a) effect of the acid type on the recovery of Mn, Li, Co and Ni under optimum conditions, (b) effect of the organic acid concentration (L-Glu) on the recovery of Li, Co, Ni and Mn under optimum conditions, (c) effect of the temperature on the recovery of Li, Co, Ni and Mn under optimum conditions, and (d) effect of the AA concentration on the recovery of Mn, Li, Co and Ni under optimum conditions.

3.1.2. Effect of the Organic Acid Concentration on the Leaching Process

Figure 1b shows the effect of the organic acid concentration on the recovery of Li, Co, Ni and Mn using L-Glu at 90 °C, an AA concentration of 0.04 M and an S/L ratio of 10 g/L for 2 h. The increase in the acid concentration from 0.1 M to 0.5 M gradually increased the

Li recovery from 79.39% to 97.05%, Co recovery from 56.58% to 75.30%, Ni recovery from 69.02% to 88.71% and Mn recovery from 62.53% to 91.26%.

Mn, Li and Ni leaching are dependent on the acidic strength and H^+ concentration, so with an increased acid concentration, the recovery increased. However, in the case of Co, despite the high effect of the H^+ concentration on its mobility, chelate formation and the conversion of Co^{3+} to Co^{2+} and complexation are crucial [48].

Above a certain concentration, with an increasing acid concentration, the effect of increasing the leaching efficiency decreases because the excess acid present in the leaching prevents the synthesis of acid anions and causes a disturbance in the acid–metal ligand and the leaching reaction. This conclusion is consistent with the work of Song et al. [1].

3.1.3. Effect of the Temperature on the Leaching Process

Figure 1c shows the effect of the temperature on the recovery of Mn, Li, Ni and Co using AA of 0.04 M, L-Glu of 0.39 M and an S/L ratio of 10 g/L for 2 h. Increasing the temperature from 30 °C to 90 °C increased the recovery of Mn, Ni, Li and Co from 66.38% to 92.22%, from 67.59% to 91.48%, from 76.52% to 98.47%, and from 49.08% to 77.91%, respectively. It is evident that the temperature is one of the parameters influencing the leaching, and at higher temperatures, the dissolution of acids and the recovery of Mn, Co, Li and Ni increases [51]. Zhang et al. found that increasing the temperature improves the average kinetic energy of the reaction and causes strong molecular collisions [52]. The increased leaching efficiency with an increasing temperature indicated that the reaction was endothermic.

3.1.4. Effect of the AA Concentration (as a Reducing Agent) on the Leaching Process

Figure 1d shows the effect of the AA concentration on the recovery of Mn, Ni, Li and Co using L-Glu at an acid concentration of 0.39 M, 90 °C, an S/L ratio of 10 g/L and 2 h.

The increase in the AA concentration increased the recovery of Mn, Ni, Li and Co from 73.60% to 92.67%, from 75.88% to 89.93%, from 72.83% to 100% and from 42.01% to 81.55%, respectively.

This efficiency increase may be attributed to the reaction of AA during the process. Because of the low Li–O bond energy, with an increasing reducing agent, the Li leaching efficiency is higher than that for Mn, Ni and Co. AA is a strong reducing agent due to its great ability to absorb molecular oxygen. Previous studies by Chen et al. and Golmohammadzadeh et al. [37,47] support these findings. The chemical bond between Co and oxygen is very strong; therefore, acidic leaching of lithium cobalt oxide ($LiCoO_2$) is difficult. Adding AA for the recovery of Co is more effective than for Ni and Mn, because the reducing agent converts insoluble Co^{3+} into soluble Co^{2+} in the leaching environment, facilitating the recovery [48].

Based on the various investigated factors affecting leaching, the optimum leaching conditions in vitro for the L-Glu + AA system, an organic acid concentration of 0.39 M, an AA concentration of 0.04 M, a temperature of 90 °C, S/L ratio of 10 g/L were determined, and for the MOA + AA system, an organic acid concentration of 0.25 M, an AA concentration of 0.03 M, a reaction temperature of 88 °C, an S/L ratio of 10 g/L and a leaching time of 2 h were determined. complete reports to investigate the optimal conditions in the MOA + AA system are reported in [48].

3.2. Characterizations

3.2.1. SEM Analysis and EDS Mapping

Figure 2 presents SEM images of the cathodic powder residues before and after leaching in the mixed acid systems (MOA + AA and L-Glu + AA) under optimal leaching conditions. As it was mentioned before, the cathode powder was subjected to a 2 h calcination at 700 °C prior to leaching. Compared to the morphology of the before leaching particles (Figure 2a), which seems crystalline, bulky and coarse, after leaching, a visible decrease in the particles' size and structure has occurred. In the MOA + AA and L-Glu + AA

leaching systems under optimum conditions, particles with a porous and irregular structure were found after leaching, indicating the proper performance of the leaching in the recovery of the cathode materials.

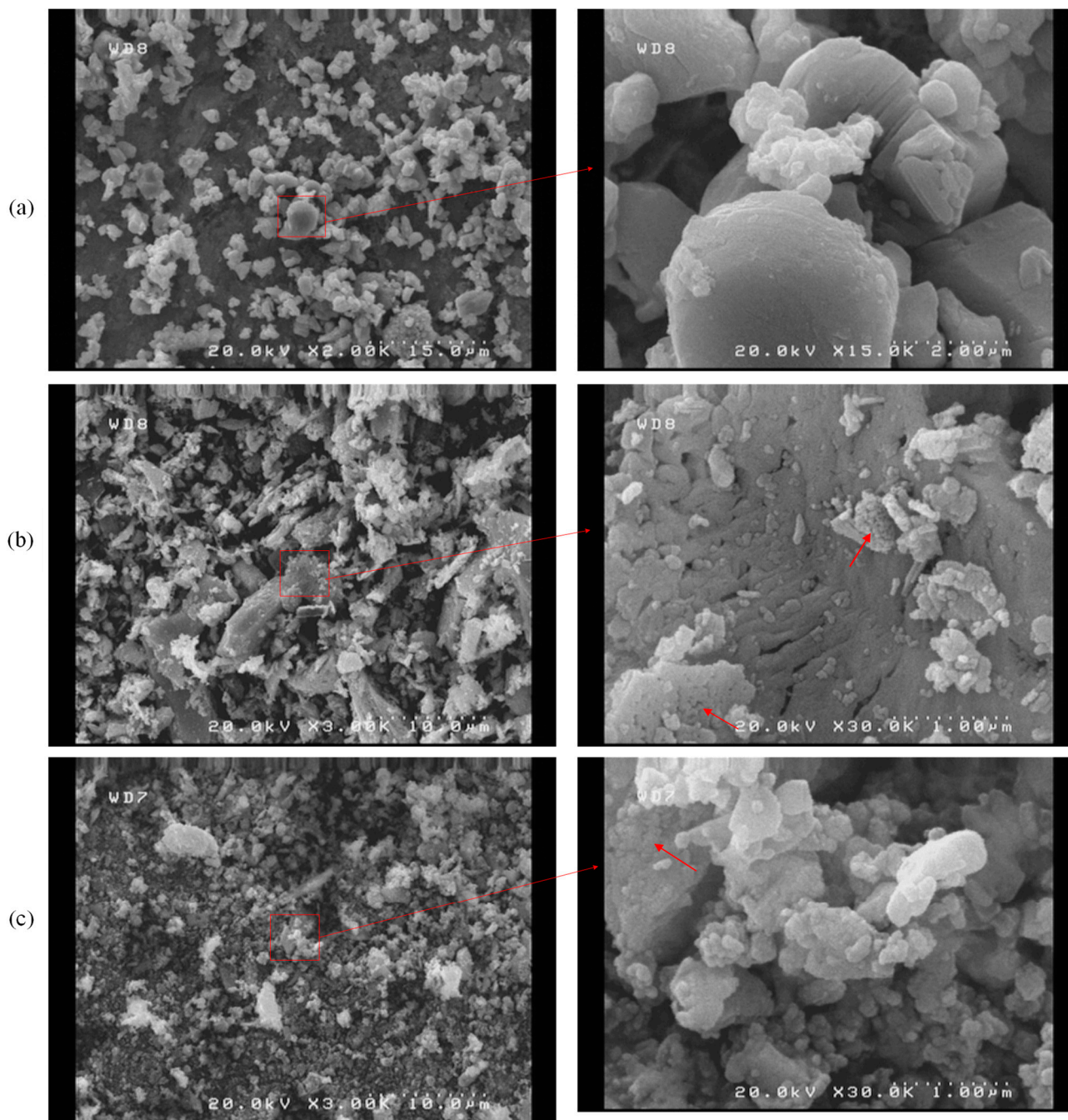


Figure 2. SEM images: (a) an LIB cathode placed in the furnace at 700 °C for 2 h, (b) the cathode material residue from leaching by MOA + AA, and (c) the cathode material residue from leaching by L-Glu + AA.

Based on the information obtained from the activation energy, the kinetic diffusion control determines the reaction rate. The ash layers after leaching confirmed the diffusion control of the leaching kinetics in the reaction with mixed acids. The ash layer after leaching is shown by the arrow in Figure 2.

Figure 3 shows the elemental map of the metals in the cathode powder, before and after leaching in the two systems (MOA + AA and L-Glu + AA) under optimum conditions.

Figure 3a shows the pre-leaching cathode powder, in which the Co, Mn, Ni and Al elements are marked with scattered, extendedly, and irregular morphology. As is clear, a high amount of the Co, Mn and Ni elements is available in the primary cathode powder. A small amount of Al appeared in the cathode in the form of impurities from the cathode sheet after crushing and sieving.

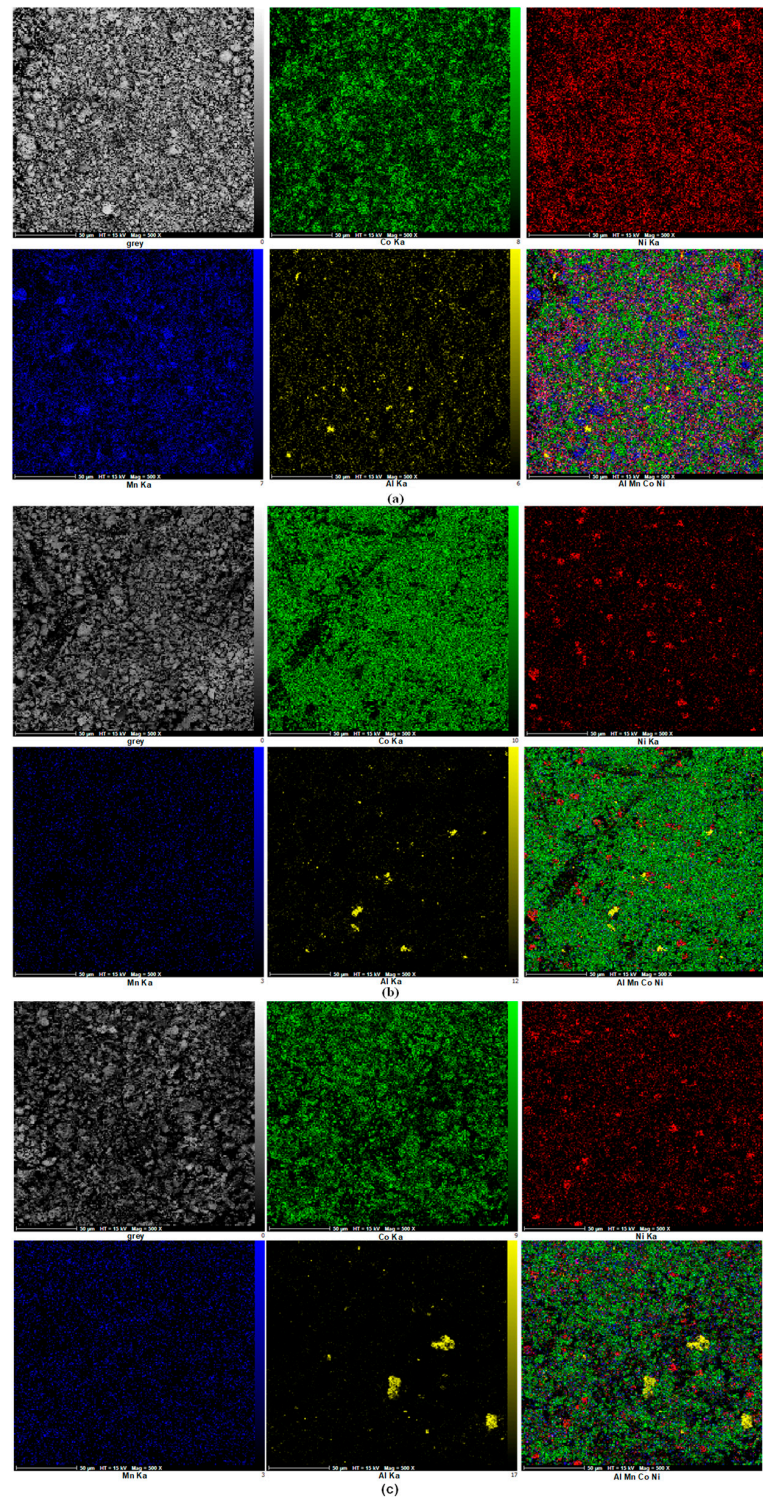


Figure 3. EDS map: (a) an LIB cathode placed in the furnace at 700 °C for 2 h, (b) the cathode material residue from leaching by MOA + AA, and (c) the cathode material residue from leaching by L-Glu + AA.

In Figure 3b,c, showing the MOA + AA and L-Glu + AA leaching system, the EDS map clearly shows a gradual decrease in the content of the metals (Mn, Co and Ni). Some Co remains in the post-leached sample due to the formation of Co_3O_4 and CoO as residual sedimentation.

3.2.2. XRD Patterns

Figure 4 shows the pattern of the leaching residues before and after calcination at $700\text{ }^\circ\text{C}$ for 2 h and after leaching in the mixed acid system (L-Glu + AA and MOA + AA) under optimum conditions. In Figure 4a, the XRD analysis of the sample before calcination shows a carbon peak that is not detectable in Figure 4b, indicating that the residual graphite would be burned during the calcination process. This is proof that the removal process for the impurities is efficient. Figure 4b indicates that the cathode material was mostly LiCoO_2 and $\text{LiNi}_{0.5}\text{Mn}_{1.5}\text{O}_4$. Figures 4c,d display the XRD analysis of the residual materials from leaching by the mixed system (MOA + AA and L-Glu + AA), where most peaks represented an insoluble species of Co_3O_4 and moreover confirmed the fact that LiCoO_2 reacted with the mixed acids (MOA + AA and L-Glu + AA) during leaching, and LiCoO_2 was leached and new species were produced.

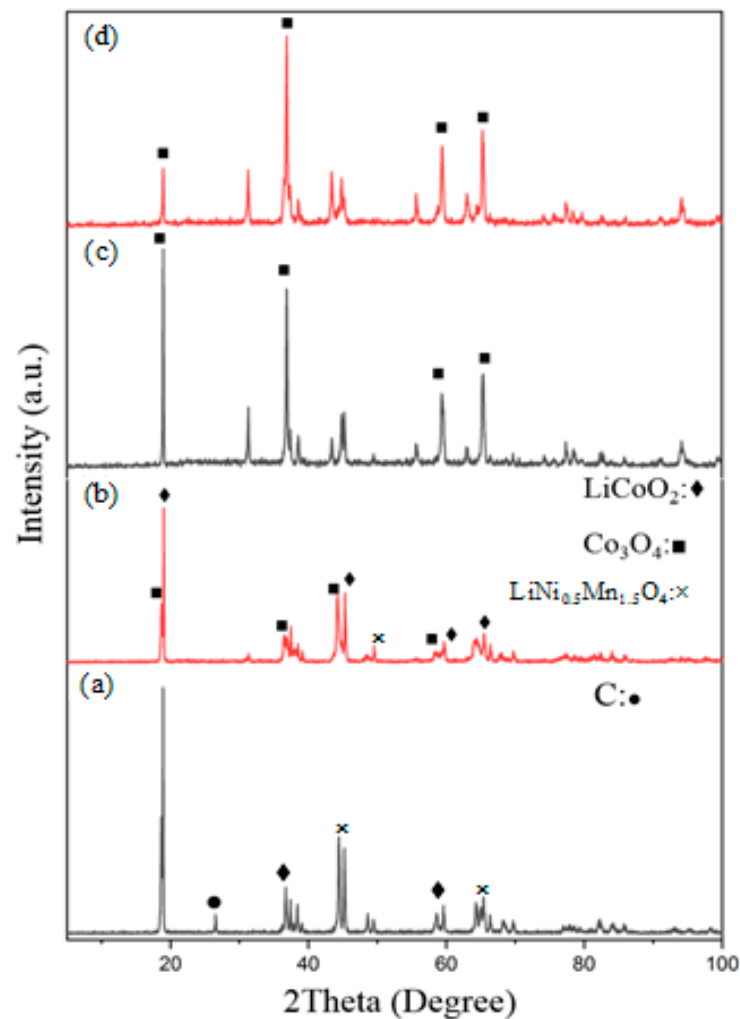


Figure 4. XRD pattern of the cathode materials before and after leaching: (a) before calcination, (b) after calcination at $700\text{ }^\circ\text{C}$ for 2 h, (c) residue of the materials after leaching by MOA + AA, and (d) residue of the materials after leaching by L-Glu + AA.

3.2.3. UV-Vis Spectrum

The UV-Vis spectrum was applied to investigate the synergistic effect of the two leaching systems, i.e., MOA and AA as well as L-Glu and AA, before and after mixing. Figure 5a displays the MOA + AA system, in which AA has two peaks of 196 and 230 nm before the reaction. After the leaching reaction of AA with the battery cathode, a widening of the AA peak and the removal of a peak were observed. These changes may be attributed to the altered intra-ligand transfers caused by the interaction with the metals. The AA peak shifted toward less energy and more wavelengths, and the structure of the ligand peak changed. In Figure 5b, which displays the L-Glu + AA system, the same thing happened to AA before and after the metal leaching. In Figure 5b, the L-Glu does not show significant absorption before leaching; however, after leaching, peaks of 387 and 531 nm indicate the formation of complexes with the metals. In these areas, ligand field transfers occurred. L-Glu formed a stronger interaction than AA, and the complex formed at 387 nm indicated the transfer of electrons from ligand to metal (and vice versa). When AA and L-Glu were used as a mixed system for leaching, the synergistic effect caused the load transfer intensity to increase due to the higher amount of material and the reducing power of AA [52]. Consequently, a stronger interaction with the metal was observed. In Figure 5a, at 500 nm of MOA, after leaching, there are ligand field transfers, complex formation, and strong interaction. MOA exhibited stronger coordination than L-Glu and acted as a reducing agent in the system. The complex formed by MOA is more stable than L-Glu, so the synergistic state has little effect on the recovery of the MOA+ AA system.

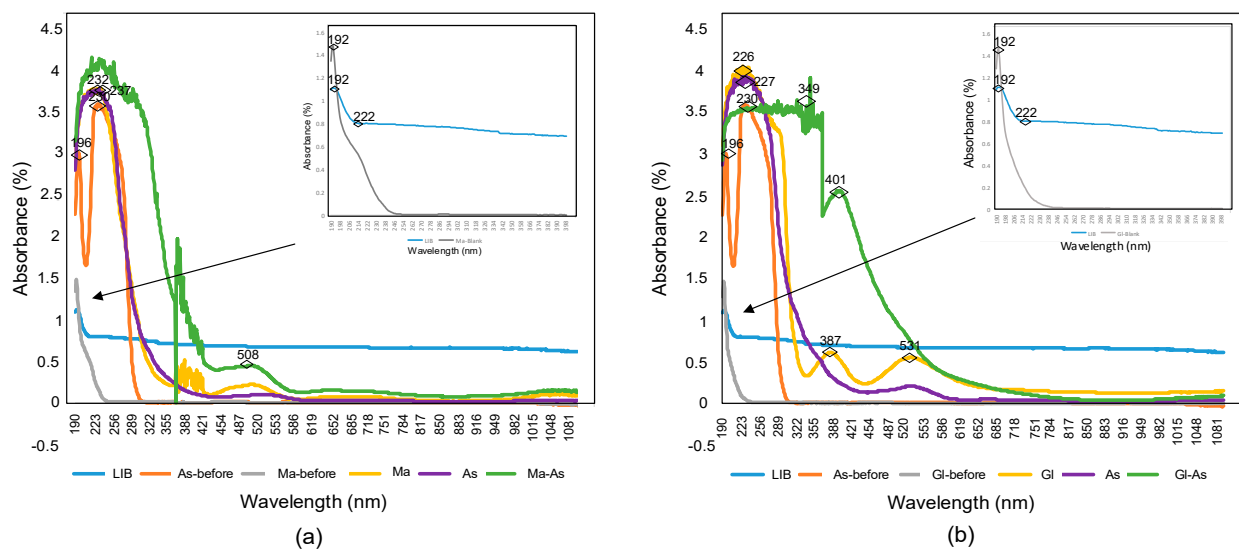


Figure 5. UV-Vis mixed acids: (a) MOA + AA before and after leaching, and (b) L-Glu + AA before and after leaching.

On the other hand, in the L-Glu + AA system, L-Glu alone was not sufficient in the reduction of Co (III) to Co (II) and required the participation of AA as a reducing agent [53]. This indicates that the synergistic state significantly affects the L-Glu + AA system.

In Figure 5b, up to 355 nm, the system has no specific absorption due to the high concentration; however, the effect of synergy is clearly observed.

3.2.4. FT-IR Spectrum

Figure 6 displays the FT-IR spectrum for an LIB cathode before and after leaching in the two different acid systems (MOA + AA and L-Glu + AA). LiCoO_2 's main spectrum includes absorption bonds of 597.37, 1026.79, 1430.79 and 3429.41. The Co–O bond absorption peak is 597.37 cm^{-1} . Changes in the intensity and width of the post-leaching Co–O peak indicated that Co dissolution occurred during leaching [13]. In Figure 6b,c, which correspond to the leaching solution in the two mixed acid systems, the peaks of 3067.13 and 3070.62 indicate

the oxidation of the functional group $-OH$ to the carboxyl or aldehyde group [45]. The infrared spectrum changed drastically from 1000 cm^{-1} to 1590 cm^{-1} , likely due to the oxidation of the hydroxyl group, leading to the formation of carboxyl or aldehyde groups. Therefore, it is concluded that this is the main area of reduction of the compounds. Peaks of 1557.25 and 1583.11 cm^{-1} are observed in the two mixed acid systems, which represent the tensile vibration of the carboxyl group, indicating that the reaction of coordination occurred during the leaching process with the AA ion. During the leaching process, the Li and soluble salts that reacted with the acid Me (Me = Mn, Co and Ni) were reduced to a highly soluble bivalent ion. AA is made up of alcohol, olefin and ester functional groups, and its two neighboring enol hydroxyl groups can readily dissociate to release H^+ . This dissociation involves the formation of conjugated systems, where the lone pair electrons of C–C, $-OH$ and C–O tend to participate. [32]. From the above observations, it is concluded that the mentioned mixed acid systems were able to form a coordination bond with the metals and change the structure of the LIB cathode.

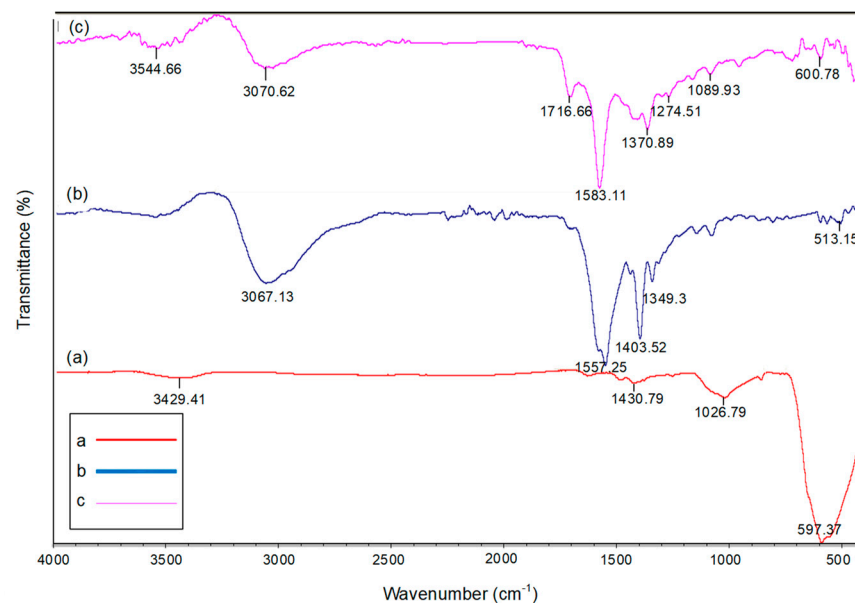


Figure 6. Infrared spectrum images: (a) the LIB cathode powder before leaching, (b) the L-Glu + AA solution system after leaching, and (c) the MOA + AA solution system after leaching.

3.3. Leaching Kinetics

The leaching of valuable metals is a process in which solid metal oxides enter the liquid phase. The reaction from the outer surface of the particles to the inner surface of the particles continues with the shrinking of the core until the reaction ends, and it is a combination of mass transfer, chemical reaction, and diffusion control [32]. The main factors affecting leaching efficiency are as follows:

- (1) Fluid Film Diffusion Control;
- (2) Ash Layer Diffusion Control;
- (3) Chemical Reaction Control of the Surface [25].

The study of leaching kinetics has an important role in identifying the rate controller stages in metal dissolution, among which the shrinking core model, the Avrami equation, the cubic rate law and the logarithmic rate law are commonly used to describe the leaching kinetics [21].

The minimum energy needed to break the bonds available during a chemical reaction is the activation energy. If the kinetic energy of the molecules is greater than this minimum energy during collision, breaking and bond formation occur (provided that the molecules collide with the appropriate orientation). The quantitative basis of the relationship between the activation energy and reaction rate is determined by the Arrhenius equation.

Kinetic studies for the purpose of metal leaching analysis were conducted in the mixed acid solution at different temperatures (30–90 °C) and leaching times (15–120 min) by keeping other factors constant: organic acid concentration (L-Glu of 0.39 M and MOA of 0.25 M), AA concentration of 0.03 M, S/L ratio of 10 g/L and time of 2 h. The leaching of metals from LiCoO₂ and LiNi_{0.5}Mn_{1.5}O₄ is a heterogeneous solid–liquid reaction and it occurs on the surface of unreactive particles.

During the leaching process, LiCoO₂ and LiNi_{0.5}Mn_{1.5}O₄ were continuously dissolved without solid phase formation. The Avrami equation was applied to describe the solid phase transfer and kinetics of the leaching reaction. The common kinetic models are as follows:

Model 1. Chemical Reaction Control of the Surface [18]:

$$1 - (1 - X)^{\frac{1}{3}} = k_1 t \quad (6)$$

Model 2. Diffusion Control [27]:

$$1 - \frac{2}{3}X - (1 - X)^{\frac{2}{3}} = k_2 t \quad (7)$$

Model 3. Logarithmic Rate Law [14]:

$$-\ln(1 - X) = k_3 t \quad (8)$$

Model 4. Avrami Equation [25,54]:

$$\ln(-\ln(1 - X)) = \ln k_4 t + \ln t \quad (9)$$

Model 5. Modified Shrinking Core [30]:

$$1 - (1 - X)^{-\frac{1}{3}} - \frac{1}{3}\ln(1 - X) = k_5 t \quad (10)$$

where X is the leaching efficiency of each metal; k_1 , k_2 , k_3 , k_4 and k_5 are the reaction rate constant from the control model (min^{-1}), t is the leaching reaction time in minutes and n is an exponential parameter.

The leaching data were fitted linearly with five models (6–10). According to the R^2 fit parameter in Table 3, Equation (9) (Avrami equation model) had a better fit correlation with the leaching data compared with the other four models. The most likely scenario was that, compared with the Avrami equation, the other four models did not well consider the change in the mass fraction of the metals in the solid phase during leaching.

The fit curves of $\ln(-\ln(1 - X))$ versus $\ln t$ show a high linear correlation for Mn, Ni, Li and Co at different temperatures, with R^2 values above 0.9 (Figures 7 and 8). The leaching process can be described by the Avrami equation with the reaction parameters, indicating that the kinetic behavior is mainly controlled by the reverse crystallization process. The n values in the mixed acid system of MOA + AA were between 0.09–0.2, and in the mixed acid system of L-Glu + AA, they were between 0.09–0.36, which confirmed that diffusion was the leaching controller in the reaction. According to Table 4, the reaction rate constant of Mn, Ni, Li and Co increased with an increasing temperature. The results showed that rising temperatures were beneficial for leaching metals from the mixed acid systems (MOA + AA and L-Glu + AA). In the mixed leaching system of MOA + AA, when the reaction temperature was similar, the Li reaction rate constant was higher in comparison with the other metals, indicating that Li leaching was faster in this system.

Table 3. Fitting parameters (R^2) of the leaching of metals in mixed acids using different models.

MOA + AA																				
T (°C)	Li					Co					Ni					Mn				
	M ₁	M ₂	M ₃	M ₄	M ₅	M ₁	M ₂	M ₃	M ₄	M ₅	M ₁	M ₂	M ₃	M ₄	M ₅	M ₁	M ₂	M ₃	M ₄	M ₅
30	0.85	0.85	0.85	0.95	0.87	0.75	0.78	0.75	0.90	0.76	0.89	0.91	0.90	0.98	0.94	0.91	0.91	0.91	0.95	0.92
50	0.95	0.95	0.95	0.90	0.95	0.88	0.86	0.88	0.94	0.88	0.74	0.75	0.76	0.91	0.82	0.72	0.73	0.74	0.90	0.78
70	0.88	0.88	0.88	0.95	0.89	0.91	0.92	0.92	0.94	0.92	0.93	0.93	0.94	0.99	0.96	0.92	0.92	0.93	0.94	0.93
88	0.93	0.97	0.97	0.94	0.97	0.98	0.98	0.98	0.96	0.99	0.85	0.85	0.89	0.97	0.93	0.91	0.91	0.93	0.96	0.96

L-Glu + AA																				
T (°C)	Li					Co					Ni					Mn				
	M ₁	M ₂	M ₃	M ₄	M ₅	M ₁	M ₂	M ₃	M ₄	M ₅	M ₁	M ₂	M ₃	M ₄	M ₅	M ₁	M ₂	M ₃	M ₄	M ₅
30	0.88	0.87	0.87	0.90	0.85	0.91	0.91	0.91	0.92	0.91	0.89	0.90	0.89	0.94	0.86	0.84	0.84	0.84	0.95	0.84
50	0.87	0.88	0.89	0.97	0.92	0.74	0.77	0.75	0.91	0.79	0.88	0.90	0.91	0.94	0.92	0.87	0.87	0.87	0.92	0.88
70	0.95	0.95	0.95	0.93	0.95	0.91	0.92	0.92	0.99	0.94	0.55	0.57	0.81	0.96	0.83	0.78	0.78	0.79	0.94	0.80
90	0.89	0.86	0.95	0.98	0.96	0.87	0.88	0.89	0.98	0.92	0.87	0.86	0.88	0.94	0.89	0.91	0.92	0.92	0.96	0.94

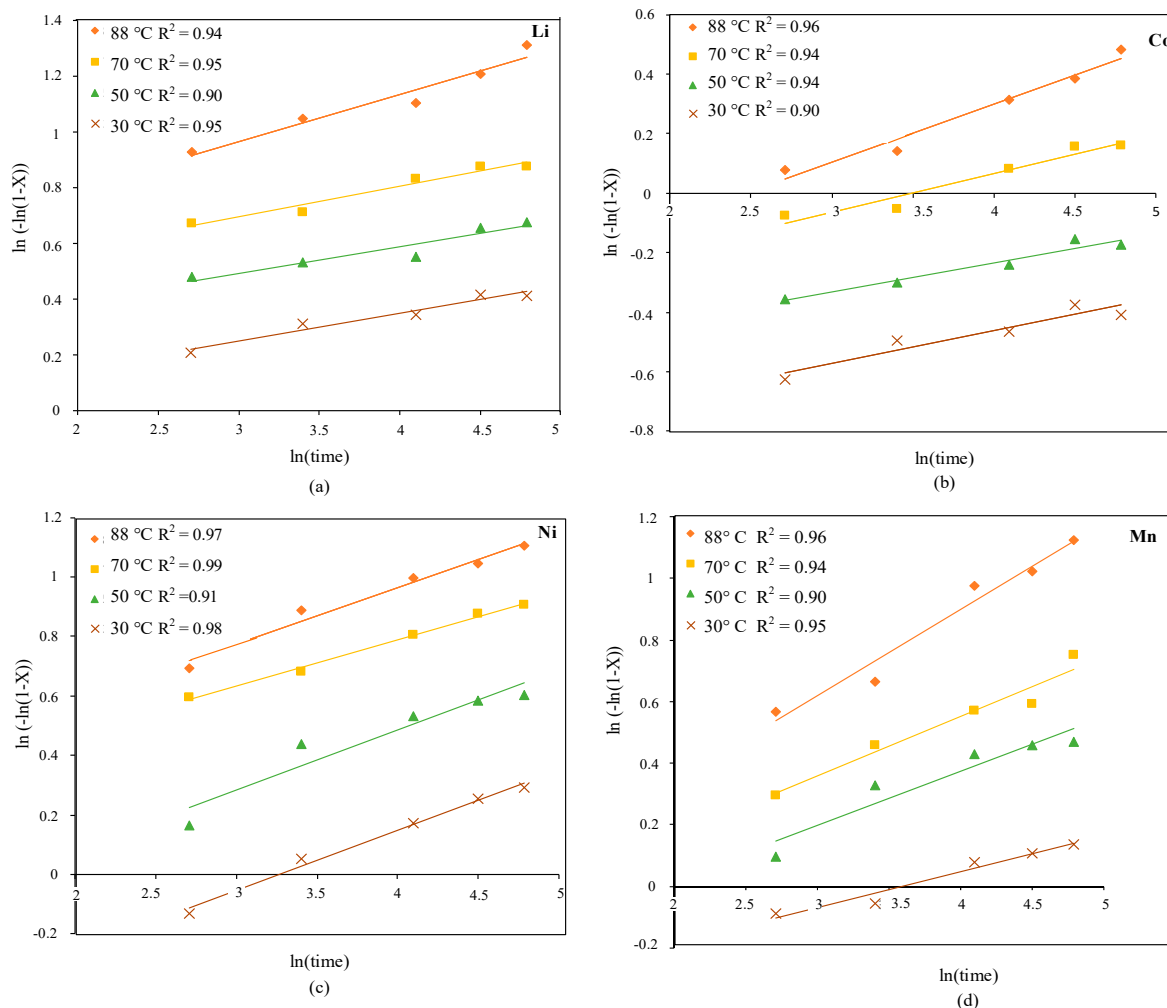


Figure 7. The results of the Avrami equation fitting of the mixed acid system (MOA + AA) at different leaching temperatures for (a) Li, (b) Co, (c) Ni and (d) Mn.

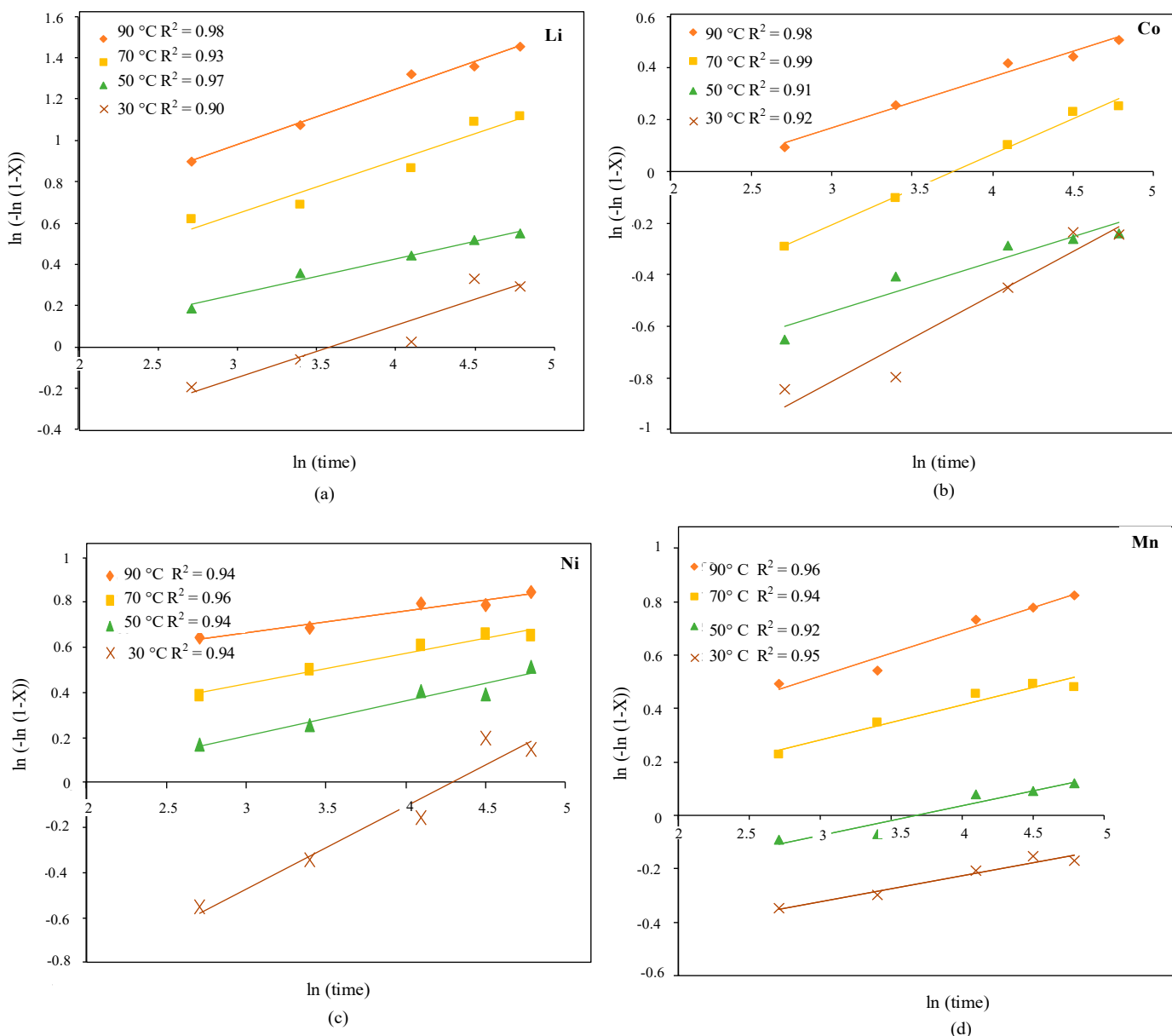


Figure 8. Avrami equation fitting of the mixed acid system (L-Glu + AA) at different leaching temperatures for (a) Li, (b) Co, (c) Ni and (d) Mn.

In addition, the Arrhenius formula is used to calculate the apparent activation energy:

$$k = Ae^{-E_a/RT} \tag{11}$$

where k is the reaction rate constant (min^{-1}), A is the pre-exponential factor, E_a is the apparent activation energy (kJ/mol), R is the global gas constant (8.314 J/K/mol) and T is the absolute temperature (K). The logarithmic form of Equation (11) is as follows:

$$\ln k = \ln A - \frac{E_a}{R} \cdot \frac{1}{T} \tag{12}$$

The $\ln k$ vs. $1/T$ diagram using the reaction rate constant (Table 4) for the mixed acid system (MOA + AA) in Figure 7 and for the mixed system (L-Glu + AA) in Figure 8 is displayed, which has a high fitness degree (>0.9).

Table 4. Parameters of the Avrami equation for Mn, Ni, Li and Co at different leaching temperatures in the two mixed acid systems.

MOA + AA								
T (°C)	Li		Co		Ni		Mn	
	n	lnk	n	lnk	n	lnk	n	lnk
30	0.098	−0.047	0.109	−0.898	0.202	−0.660	0.116	−0.417
50	0.094	0.208	0.097	−0.625	0.201	−0.323	0.174	−0.324
70	0.110	0.362	0.129	−0.452	0.155	0.169	0.194	−0.223
88	0.169	0.455	0.195	−0.480	0.189	0.208	0.281	−0.225
L-Glu + AA								
T (°C)	Li		Co		Ni		Mn	
	n	lnk	n	lnk	n	lnk	n	lnk
30	0.252	−0.906	0.335	−1.820	0.368	−1.578	0.096	−0.612
50	0.169	−0.251	0.193	−1.125	0.157	−0.269	0.111	−0.411
70	0.258	−0.129	0.273	−1.026	0.135	0.0327	0.130	−0.109
90	0.269	0.171	0.196	−0.422	0.097	0.374	0.170	0.009

The apparent activation energy (kJ/mol) in the mixed system (MOA + AA) for Mn, Ni, Li and Co was 3.23, 14.72, 7.36 and 7.77, respectively, indicating that the leaching process involved diffusion control (Figure 9). In the mixed acid system (L-Glu + AA), the apparent activation energy (kJ/mol) for Mn, Ni, Co and Li was 9.95, 29.42, 20.15 and 16.01, respectively (Figure 9), which means that the dissolution of the battery cathode in the acid system of the mixture simultaneously followed the chemical reaction and the diffusion control mechanisms; however, the effect of the diffusion control mechanism was greater than the chemical control because the activation energy for these reactions was closer to the diffusion control.

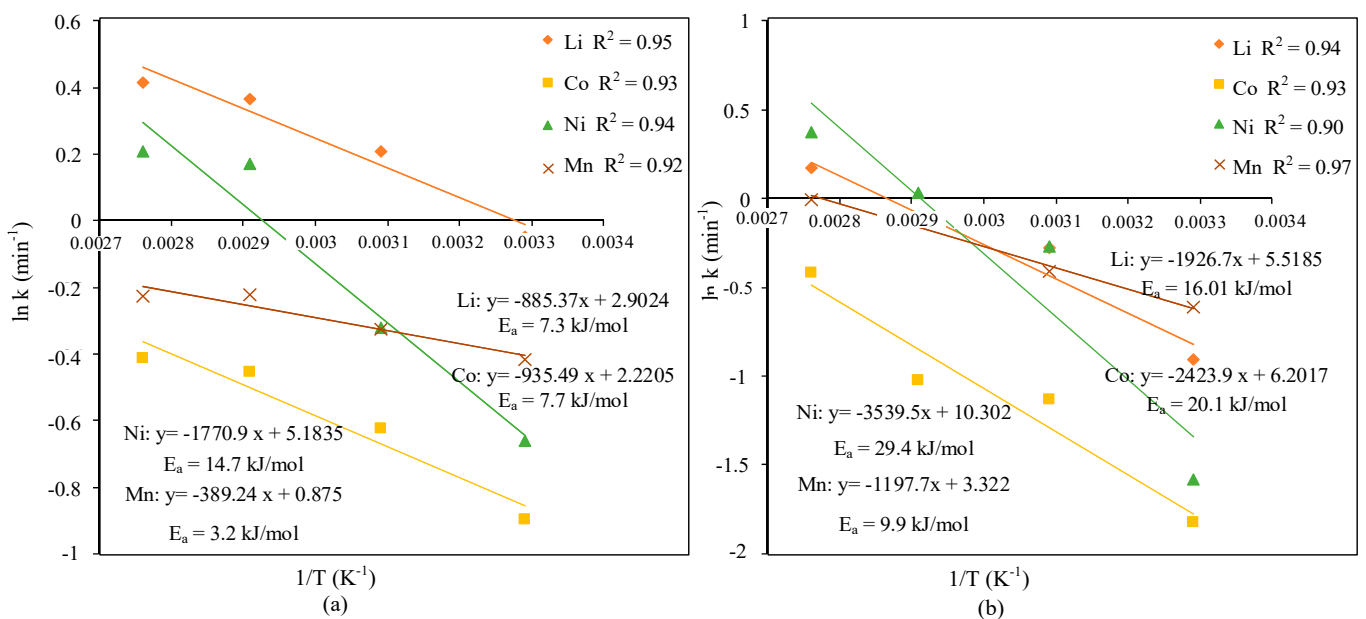


Figure 9. Arrhenius design for leaching Li, Co, Ni and Mn from spent LIBs: (a) system MOA + AA, and (b) system L-Glu + AA.

In the diagram of the Arrhenius equation, the reactions with higher activation energy contain a steeper slope and the reaction rate is highly sensitive to the temperature change. In

contrast, reactions with lower activation energy are less sensitive to the temperature change. As shown in Figure 9b, which corresponds to the mixed acid system (L-Glu + AA), due to the higher activation energy compared with the MOA + AA mixture system (Figure 9a), the slope of the graphs was steeper, which confirms the fact mentioned. The activation energy of the reaction was closely related to its rate, i.e., the higher the activation energy, the slower the chemical reaction. This occurs due to the fact that the molecules can only complete the reaction when they reach the top of the energy activation barrier. The higher the activation energy, the fewer molecules with enough energy to pass through at any given moment.

The observations indicated that spent LIB's cathode was dissolved easier in the mixed acid system (MOA + AA) than (L-Glu + AA), which was due to the lower activation energy. Moreover, the activation energy for Li and Mn was lower than for Co and Ni, indicating that it was easier to remove Li from the LiCoO_2 structure and Mn from the $\text{LiNi}_{0.5}\text{Mn}_{1.5}\text{O}_4$ structure. The difference between the activation energies of the transition metals is related to the polyvalent properties of Ni and Co.

In Refs. [1,32], through research of review articles and the structural characteristics of materials, the authors propose the following mechanism and possible leaching products. The leaching of MOA and L-Glu acids using LiCoO_2 and $\text{LiNi}_{0.5}\text{Mn}_{1.5}\text{O}_4$ cathode powder is displayed in Figure 10.

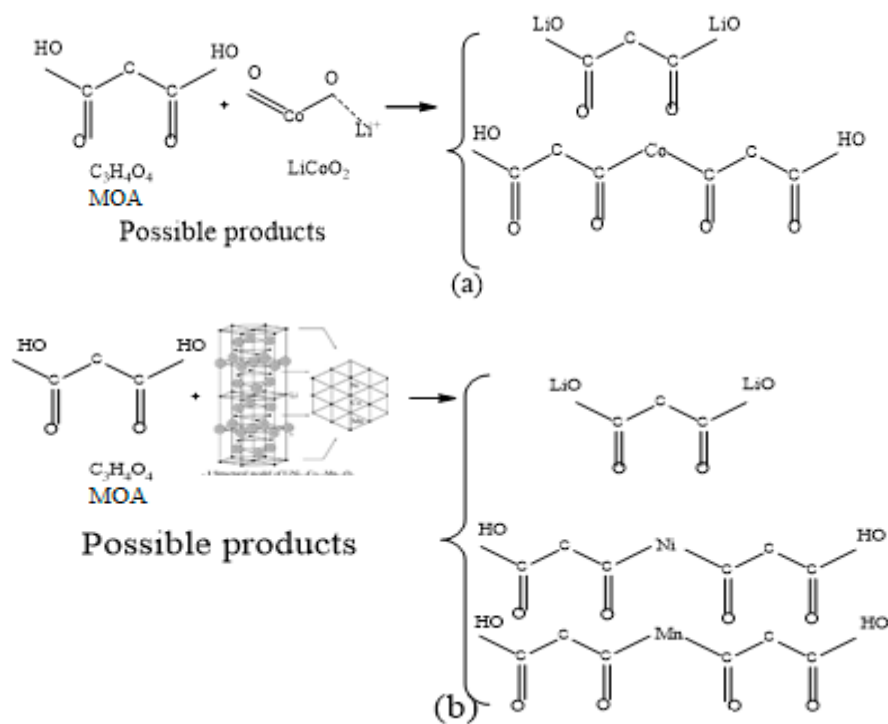


Figure 10. Cont.

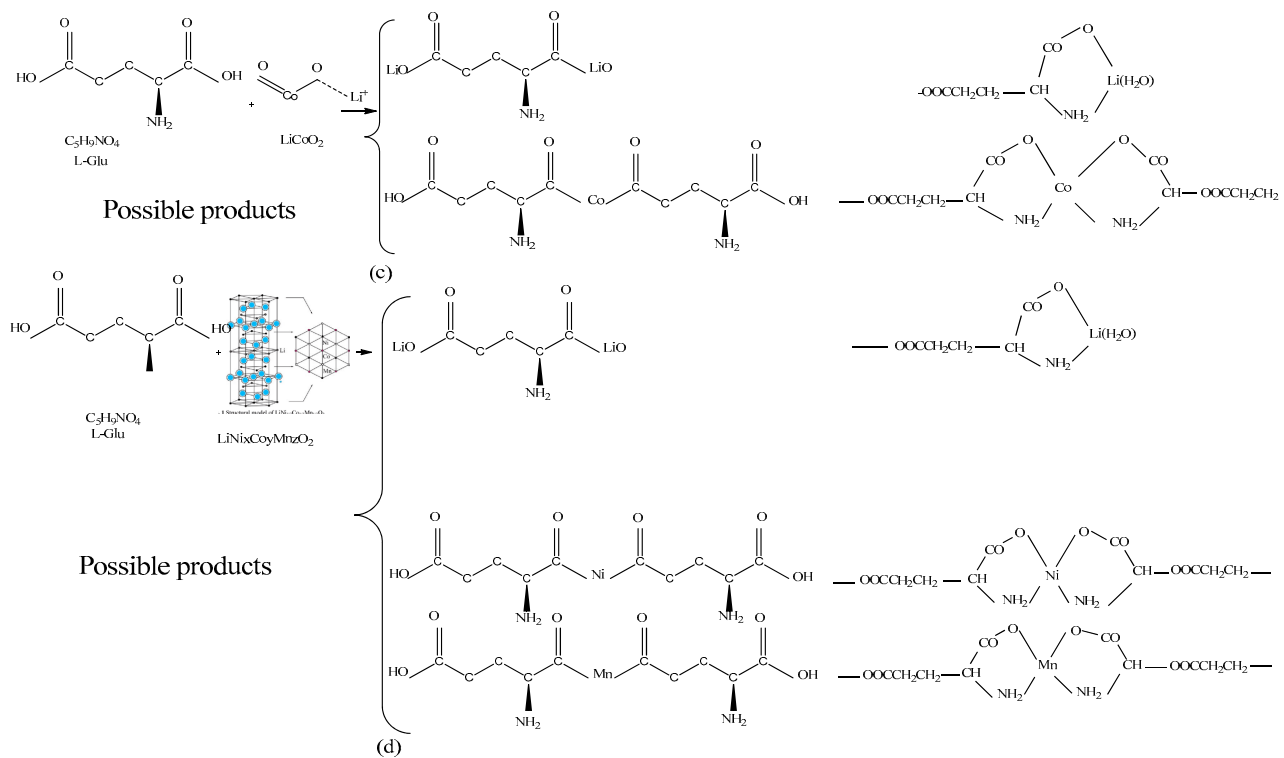


Figure 10. Leaching mechanism: (a) system MOA + AA with LiCoO_2 , (b) system MOA + AA with $\text{LiNi}_{0.5}\text{Mn}_{1.5}\text{O}_4$, (c) system L-Glu + AA with LiCoO_2 , and (d) system L-Glu + AA with $\text{LiNi}_{0.5}\text{Mn}_{1.5}\text{O}_4$.

4. Conclusions

In this research, a fresh hydrometallurgical process was proposed for leaching cathode materials from spent LIBs using two mixed acid systems (MOA + AA and L-Glu + AA). Using the MOA + AA system, high leaching recovery percentages were possible for Li (100%), Co (80%), Ni (99%), and Mn (98%) considering the optimized conditions, including the temperature of 88 °C, MOA concentration of 0.25 M, AA concentration of 0.03 M, reaction time of 2 h, and S/L ratio of 10 g/L. The leaching recovery for L-Glu + AA system was found to be slightly lower, as Li (100%), Co (79%), Ni (91%) and Mn (92%) under optimum conditions occurred at the temperature of 90 °C, L-Glu concentration of 0.39 M, AA concentration of 0.04 M, reaction time of 2 h and S/L ratio of 10 g/L. Due to the lower acid consumption and greater recovery, the MOA + AA system was more suitable for metal recovery. The Avrami equation provided the best fit with the leaching kinetics of the LIB cathode in the mixed acid system. The apparent activation energy (kJ/mol) in the MOA + AA system for Mn, Ni, Li and Co was 3.23, 14.72, 7.36 and 7.77, respectively, which indicated that the leaching process was a diffusion control. The apparent activation energy (kJ/mol) in the L-Glu + AA system for Mn, Ni, Li and Co was 9.95, 29.42, 16.08 and 20.15, respectively, and indicated that they followed chemical reaction and diffusion control mechanisms simultaneously; however, the effect of the diffusion control mechanism was greater than the chemical reaction. According to the analytical results, the synergistic effect in the L-Glu + AA system was more significant in comparison with the MOA + AA system. MOA was more strongly coordinated, and it reduced the system, so it caused higher recovery and was not affected by AA to achieve significant results; however, L-Glu was not able to reduce the system and AA was required to recover it. This leaching method is environmentally friendly and moreover cost-effective for recovering valuable metals from spent LIB cathodes.

Author Contributions: L.S. and S.Z.S.T. conceived and planned the experiments. L.S. carried out the experiments. S.Z.S.T. and A.E.-Z. contributed to the interpretation of the results. A.E.-Z. and L.S. took the lead in writing and editing the manuscript. S.Z.S.T. and M.N. were supervisor. All authors provided critical feedback and helped shape the research, analysis, and manuscript. All authors have read and agreed to the published version of the manuscript.

Funding: This research received no external funding.

Data Availability Statement: Data is contained within the article.

Conflicts of Interest: The authors declare no conflict of interest.

References

1. Song, D.; Wang, T.; Liu, Z.; Zhao, S.; Quan, J.; Li, G.; Zhu, H.; Huang, J.; He, W. Characteristic comparison of leaching valuable metals from spent power Li-ion batteries for vehicles using the inorganic and organic acid system. *J. Environ. Chem. Eng.* **2022**, *10*, 107102. [[CrossRef](#)]
2. Zhang, X.; Cai, L.; Fan, E.; Lin, J.; Wu, F.; Chen, R.; Li, L. Recovery valuable metals from spent lithium-ion batteries via a low-temperature roasting approach: Thermodynamics and conversion mechanism. *J. Hazard. Mater. Adv.* **2021**, *1*, 100003. [[CrossRef](#)]
3. Xia, X.; Li, P. A review of the life cycle assessment of electric vehicles: Considering the influence of batteries. *Sci. Total Environ.* **2022**, *814*, 152870. [[CrossRef](#)] [[PubMed](#)]
4. Jung, J.C.-Y.; Sui, P.-C.; Zhang, J. A review of recycling spent lithium-ion battery cathode materials using hydrometallurgical treatments. *J. Energy Storage* **2021**, *35*, 102217. [[CrossRef](#)]
5. Tang, X.; Tang, W.; Duan, J.; Yang, W.; Wang, R.; Tang, M.; Li, J. Recovery of valuable metals and modification of cathode materials from spent lithium-ion batteries. *J. Alloys Compd.* **2021**, *874*, 159853. [[CrossRef](#)]
6. Weshahy, A.R.; Gouda, A.A.; Atia, B.M.; Sakr, A.K.; Al-Otaibi, J.S.; Almuqrin, A.; Hanfi, M.Y.; Sayyed, M.; El Sheikh, R.; Radwan, H.A. Efficient Recovery of Rare Earth Elements and Zinc from Spent Ni–Metal Hydride Batteries: Statistical Studies. *Nanomaterials* **2022**, *12*, 2305. [[CrossRef](#)] [[PubMed](#)]
7. Li, P.; Xia, X.; Guo, J. A review of the life cycle carbon footprint of electric vehicle batteries. *Sep. Purif. Technol.* **2022**, *296*, 121389. [[CrossRef](#)]
8. Zheng, Q.; Watanabe, M.; Iwatate, Y.; Azuma, D.; Shibasaki, K.; Hiraga, Y.; Kishita, A.; Nakayasu, Y. Hydrothermal leaching of ternary and binary lithium-ion battery cathode materials with citric acid and the kinetic study. *J. Supercrit. Fluids* **2020**, *165*, 104990. [[CrossRef](#)]
9. Verma, A.; Corbin, D.R.; Shiflett, M.B. Lithium and cobalt recovery for lithium-ion battery recycle using an improved oxalate process with hydrogen peroxide. *Hydrometallurgy* **2021**, *203*, 105694. [[CrossRef](#)]
10. Sommerville, R.; Zhu, P.; Rajaeifar, M.A.; Heidrich, O.; Goodship, V.; Kendrick, E. A qualitative assessment of lithium ion battery recycling processes. *Resour. Conserv. Recycl.* **2021**, *165*, 105219. [[CrossRef](#)]
11. Chen, M.; Wang, R.; Qi, Y.; Han, Y.; Wang, R.; Fu, J.; Meng, F.; Yi, X.; Huang, J.; Shu, J. Cobalt and lithium leaching from waste lithium ion batteries by glycine. *J. Power Sources* **2021**, *482*, 228942. [[CrossRef](#)]
12. Lie, J.; Liu, J.-C. Closed-vessel microwave leaching of valuable metals from spent lithium-ion batteries (LIBs) using dual-function leaching agent: Ascorbic acid. *Sep. Purif. Technol.* **2021**, *266*, 118458. [[CrossRef](#)]
13. Zhou, S.; Zhang, Y.; Meng, Q.; Dong, P.; Fei, Z.; Li, Q. Recycling of LiCoO₂ cathode material from spent lithium ion batteries by ultrasonic enhanced leaching and one-step regeneration. *J. Environ. Manag.* **2021**, *277*, 111426. [[CrossRef](#)] [[PubMed](#)]
14. Chabhadiya, K.; Srivastava, R.R.; Pathak, P. Two-step leaching process and kinetics for an eco-friendly recycling of critical metals from spent Li-ion batteries. *J. Environ. Chem. Eng.* **2021**, *9*, 105232. [[CrossRef](#)]
15. Liu, P.; Xiao, L.; Chen, Y.; Tang, Y.; Wu, J.; Chen, H. Recovering valuable metals from LiNixCoyMn1-x-yO₂ cathode materials of spent lithium ion batteries via a combination of reduction roasting and stepwise leaching. *J. Alloys Compd.* **2019**, *783*, 743–752. [[CrossRef](#)]
16. Ning, P.; Meng, Q.; Dong, P.; Duan, J.; Xu, M.; Lin, Y.; Zhang, Y. Recycling of cathode material from spent lithium ion batteries using an ultrasound-assisted DL-malic acid leaching system. *Waste Manag.* **2020**, *103*, 52–60. [[CrossRef](#)] [[PubMed](#)]
17. Ma, Y.; Tang, J.; Wanaldi, R.; Zhou, X.; Wang, H.; Zhou, C.; Yang, J. A promising selective recovery process of valuable metals from spent lithium ion batteries via reduction roasting and ammonia leaching. *J. Hazard. Mater.* **2021**, *402*, 123491. [[CrossRef](#)]
18. Wu, C.; Li, B.; Yuan, C.; Ni, S.; Li, L. Recycling valuable metals from spent lithium-ion batteries by ammonium sulfite-reduction ammonia leaching. *Waste Manag.* **2019**, *93*, 153–161. [[CrossRef](#)]
19. Musariri, B.; Akdogan, G.; Dorfling, C.; Bradshaw, S. Evaluating organic acids as alternative leaching reagents for metal recovery from lithium ion batteries. *Miner. Eng.* **2019**, *137*, 108–117. [[CrossRef](#)]
20. Xiao, J.; Niu, B.; Song, Q.; Zhan, L.; Xu, Z. Novel targetedly extracting lithium: An environmental-friendly controlled chlorinating technology and mechanism of spent lithium ion batteries recovery. *J. Hazard. Mater.* **2021**, *404*, 123947. [[CrossRef](#)]
21. Fu, Y.; He, Y.; Li, J.; Qu, L.; Yang, Y.; Guo, X.; Xie, W. Improved hydrometallurgical extraction of valuable metals from spent lithium-ion batteries via a closed-loop process. *J. Alloys Compd.* **2020**, *847*, 156489. [[CrossRef](#)]

22. Weshahy, A.R.; Sakr, A.K.; Gouda, A.A.; Atia, B.M.; Somaily, H.; Hanfi, M.Y.; Sayyed, M.; El Sheikh, R.; El-Sheikh, E.M.; Radwan, H.A. Selective recovery of cadmium, cobalt, and nickel from spent Ni–Cd batteries using Adogen®464 and mesoporous silica derivatives. *Int. J. Mol. Sci.* **2022**, *23*, 8677. [[CrossRef](#)] [[PubMed](#)]
23. Barik, S.; Prabakaran, G.; Kumar, L. Leaching and separation of Co and Mn from electrode materials of spent lithium-ion batteries using hydrochloric acid: Laboratory and pilot scale study. *J. Clean. Prod.* **2017**, *147*, 37–43. [[CrossRef](#)]
24. Peng, C.; Hamuyuni, J.; Wilson, B.P.; Lundström, M. Selective reductive leaching of cobalt and lithium from industrially crushed waste Li-ion batteries in sulfuric acid system. *Waste Manag.* **2018**, *76*, 582–590. [[CrossRef](#)] [[PubMed](#)]
25. Zhuang, L.; Sun, C.; Zhou, T.; Li, H.; Dai, A. Recovery of valuable metals from LiNi_{0.5}Co_{0.2}Mn_{0.3}O₂ cathode materials of spent Li-ion batteries using mild mixed acid as leachant. *Waste Manag.* **2019**, *85*, 175–185. [[CrossRef](#)] [[PubMed](#)]
26. Munir, H.; Srivastava, R.R.; Kim, H.; Ilyas, S.; Khosa, M.K.; Yameen, B. Leaching of exhausted LNCM cathode batteries in ascorbic acid lixiviant: A green recycling approach, reaction kinetics and process mechanism. *J. Chem. Technol. Biotechnol.* **2020**, *95*, 2286–2294. [[CrossRef](#)]
27. Natarajan, S.; Boricha, A.B.; Bajaj, H.C. Recovery of value-added products from cathode and anode material of spent lithium-ion batteries. *Waste Manag.* **2018**, *77*, 455–465. [[CrossRef](#)] [[PubMed](#)]
28. Zhang, X.; Bian, Y.; Xu, S.; Fan, E.; Xue, Q.; Guan, Y.; Wu, F.; Li, L.; Chen, R. Innovative application of acid leaching to regenerate Li (Ni_{1/3}Co_{1/3}Mn_{1/3}) O₂ cathodes from spent lithium-ion batteries. *ACS Sustain. Chem. Eng.* **2018**, *6*, 5959–5968. [[CrossRef](#)]
29. Li, D.; Zhang, B.; Ou, X.; Zhang, J.; Meng, K.; Ji, G.; Li, P.; Xu, J. Ammonia leaching mechanism and kinetics of LiCoO₂ material from spent lithium-ion batteries. *Chin. Chem. Lett.* **2021**, *32*, 2333–2337. [[CrossRef](#)]
30. Fu, Y.; He, Y.; Qu, L.; Feng, Y.; Li, J.; Liu, J.; Zhang, G.; Xie, W. Enhancement in leaching process of lithium and cobalt from spent lithium-ion batteries using benzenesulfonic acid system. *Waste Manag.* **2019**, *88*, 191–199. [[CrossRef](#)]
31. Zhang, X.; Li, L.; Fan, E.; Xue, Q.; Bian, Y.; Wu, F.; Chen, R. Toward sustainable and systematic recycling of spent rechargeable batteries. *Chem. Soc. Rev.* **2018**, *47*, 7239–7302. [[CrossRef](#)] [[PubMed](#)]
32. Yan, S.; Sun, C.; Zhou, T.; Gao, R.; Xie, H. Ultrasonic-assisted leaching of valuable metals from spent lithium-ion batteries using organic additives. *Sep. Purif. Technol.* **2021**, *257*, 117930. [[CrossRef](#)]
33. Meshram, P.; Pandey, B.; Mankhand, T. Hydrometallurgical processing of spent lithium ion batteries (LIBs) in the presence of a reducing agent with emphasis on kinetics of leaching. *Chem. Eng. J.* **2015**, *281*, 418–427. [[CrossRef](#)]
34. Chen, X.; Guo, C.; Ma, H.; Li, J.; Zhou, T.; Cao, L.; Kang, D. Organic reductants based leaching: A sustainable process for the recovery of valuable metals from spent lithium ion batteries. *Waste Manag.* **2018**, *75*, 459–468. [[CrossRef](#)] [[PubMed](#)]
35. Zhang, Y.; Meng, Q.; Dong, P.; Duan, J.; Lin, Y. Use of grape seed as reductant for leaching of cobalt from spent lithium-ion batteries. *J. Ind. Eng. Chem.* **2018**, *66*, 86–93. [[CrossRef](#)]
36. Sahu, S.; Pati, S.; Devi, N. A Detailed Kinetic Analysis of the Environmentally Friendly Leaching of Spent Lithium-Ion Batteries Using Monocarboxylic Acid. *Metals* **2023**, *13*, 947. [[CrossRef](#)]
37. Cerrillo-Gonzalez, M.d.M.; Villen-Guzman, M.; Vereda-Alonso, C.; Rodriguez-Maroto, J.M.; Paz-Garcia, J.M. Acid leaching of LiCoO₂ enhanced by reducing agent. Model formulation and validation. *Chemosphere* **2022**, *287*, 132020. [[CrossRef](#)]
38. Xiao, X.; Hoogendoorn, B.W.; Ma, Y.; Sahadevan, S.A.; Gardner, J.M.; Forsberg, K.; Olsson, R.T. Ultrasound-assisted extraction of metals from Lithium-ion batteries using natural organic acids. *Green Chem.* **2021**, *23*, 8519–8532. [[CrossRef](#)]
39. Islam, A.; Roy, S.; Khan, M.A.; Mondal, P.; Teo, S.H.; Taufiq-Yap, Y.H.; Ahmed, M.T.; Choudhury, T.R.; Abdulkreem-Alsultan, G.; Khandaker, S. Improving valuable metal ions capturing from spent Li-ion batteries with novel materials and approaches. *J. Mol. Liq.* **2021**, *338*, 116703. [[CrossRef](#)]
40. Meng, F.; Liu, Q.; Kim, R.; Wang, J.; Liu, G.; Ghahreman, A. Selective recovery of valuable metals from industrial waste lithium-ion batteries using citric acid under reductive conditions: Leaching optimization and kinetic analysis. *Hydrometallurgy* **2020**, *191*, 105160. [[CrossRef](#)]
41. Sung, M.H.; Park, C.; Kim, C.J.; Poo, H.; Soda, K.; Ashiuchi, M. Natural and edible biopolymer poly- γ -glutamic acid: Synthesis, production, and applications. *Chem. Rec.* **2005**, *5*, 352–366. [[CrossRef](#)] [[PubMed](#)]
42. Kettler, R.M.; Wesolowski, D.J.; Palmer, D.A. Dissociation quotients of malonic acid in aqueous sodium chloride media to 100 C. *J. Solut. Chem.* **1992**, *21*, 883–900. [[CrossRef](#)]
43. Zheng, Y.; Song, W.; Mo, W.-T.; Zhou, L.; Liu, J.-W. Lithium fluoride recovery from cathode material of spent lithium-ion battery. *RSC Adv.* **2018**, *8*, 8990–8998. [[CrossRef](#)] [[PubMed](#)]
44. Ku, H.; Jung, Y.; Jo, M.; Park, S.; Kim, S.; Yang, D.; Rhee, K.; An, E.-M.; Sohn, J.; Kwon, K. Recycling of spent lithium-ion battery cathode materials by ammoniacal leaching. *J. Hazard. Mater.* **2016**, *313*, 138–146. [[CrossRef](#)] [[PubMed](#)]
45. Zhu, B.; Zhang, Y.; Zou, Y.; Yang, Z.; Zhang, B.; Zhao, Y.; Zhang, M.; Meng, Q.; Dong, P. Leaching kinetics and interface reaction of LiNi_{0.6}Co_{0.2}Mn_{0.2}O₂ materials from spent LIBs using GKB as reductant. *J. Environ. Manag.* **2021**, *300*, 113710. [[CrossRef](#)]
46. Gao, W.; Liu, C.; Cao, H.; Zheng, X.; Lin, X.; Wang, H.; Zhang, Y.; Sun, Z. Comprehensive evaluation on effective leaching of critical metals from spent lithium-ion batteries. *Waste Manag.* **2018**, *75*, 477–485. [[CrossRef](#)] [[PubMed](#)]
47. Dutta, D.; Kumari, A.; Panda, R.; Jha, S.; Gupta, D.; Goel, S.; Jha, M.K. Close loop separation process for the recovery of Co, Cu, Mn, Fe and Li from spent lithium-ion batteries. *Sep. Purif. Technol.* **2018**, *200*, 327–334. [[CrossRef](#)]
48. Sohbatzadeh, L.; Shafaei Tonkaboni, S.Z.; Noaparast, M. An Environmentally Friendly Method for Recovery of Metals from Cathode Material of Lithium-Ion Batteries using L-Glutamic, Malonic, and Ascorbic acid. *J. Min. Environ.* **2022**, *13*, 1171–1188.

49. Hamborg, E.S.; Niederer, J.P.; Versteeg, G.F. Dissociation constants and thermodynamic properties of amino acids used in CO₂ absorption from (293 to 353) K. *J. Chem. Eng. Data* **2007**, *52*, 2491–2502. [[CrossRef](#)]
50. DeRuiter, J. Carboxylic acid structure and chemistry: Part 1. *Princ. Drug Action* **2005**, *1*, 1–10.
51. Su, F.; Meng, Q.; Zhou, X.; Liu, X.; Yang, J.; Tang, J.; Yang, W.; Cao, P.; Li, Z.; Wang, H. One-step leaching mechanism for total elemental recovery from spent lithium-ion batteries utilizing ethylene diamine tetraacetic acid. *J. Environ. Chem. Eng.* **2023**, *11*, 110275. [[CrossRef](#)]
52. Zhang, J.; Hu, X.; He, T.; Yuan, X.; Li, X.; Shi, H.; Yang, L.; Shao, P.; Wang, C.; Luo, X. Rapid extraction of valuable metals from spent LiNixCoyMn1-x-yO2 cathodes based on synergistic effects between organic acids. *Waste Manag.* **2023**, *165*, 19–26. [[CrossRef](#)] [[PubMed](#)]
53. Nayaka, G.; Pai, K.; Santhosh, G.; Manjanna, J. Dissolution of cathode active material of spent Li-ion batteries using tartaric acid and ascorbic acid mixture to recover Co. *Hydrometallurgy* **2016**, *161*, 54–57. [[CrossRef](#)]
54. Choi, J.-W.; Cho, C.-W.; Yun, Y.-S. Organic acid-based linear free energy relationship models for green leaching of strategic metals from spent lithium-ion batteries and improvement of leaching performance. *J. Hazard. Mater.* **2022**, *423*, 127214. [[CrossRef](#)]

Disclaimer/Publisher's Note: The statements, opinions and data contained in all publications are solely those of the individual author(s) and contributor(s) and not of MDPI and/or the editor(s). MDPI and/or the editor(s) disclaim responsibility for any injury to people or property resulting from any ideas, methods, instructions or products referred to in the content.